INORGANIC CHEMISTRY
FRONTIERS

CHEMISTRY FRONTIERS

View Article Online
View Journal | View Issue



Cite this: *Inorg. Chem. Front.*, 2024, **11**, 1313

# Magneto-chiral dichroism of chiral lanthanide complexes

Fabrice Pointillart, *[a] Matteo Atzori *[b] and Cyrille Train [b]

Magneto-Chiral Dichroism (MChD) is an enantioselective and polarization independent light–matter interaction shown by magnetized chiral molecules and materials. This phenomenon, predicted in 1984 and experimentally demonstrated in 1997 by studying the differential visible light emission of a chiral $Eu^{III}$ complex, is now attracting the interest of the chemical community working with transition metal and lanthanide-based chiral complexes. This is motivated by both the information on the magnetic, electronic and chiroptical properties that can be retrieved using this unconventional spectroscopic technique and the potential technological applications that can be foreseen, such as the optical readout of magnetic data without the need for polarization-based readout devices. In particular, chiral lanthanide complexes, which intrinsically have high spin–orbit coupling (a key factor to observe MChD), a variety of electronic configurations, a multitude of electronic transitions of different characteristics, variable coordination geometries and different degrees of magnetic anisotropy, represent ideal molecules to investigate MChD in both light absorption and emission in a wide spectral range. This perspective summarizes the studies reported so far in the literature on the MChD of chiral lanthanide complexes and provides some general conclusions that will help the chemical community in designing lanthanide-based systems highly responsive to MChD. Finally, we suggest prospective experiments and studies that are needed to push forward the understanding and the use of this fascinating phenomenon.

Received 6th December 2023,
Accepted 30th January 2024

DOI: 10.1039/d3qi02510a

rsc.li/frontiers-inorganic



## Introduction

Chirality represents the possibility for an object to exist as two non-superposable mirror images forming a pair of enantiomers.[1] Such a structural property is extremely relevant for a multitude of scientific aspects in chemistry, biology and physics.[1,2] One of the most known properties of chiral objects is their ability to rotate the plane of light polarization (Natural Optical Activity, NOA) with a rotatory sign (*dextro* or *levo*) dependent on the absolute configuration of the system.[3] Optical manifestations related to NOA are Natural Circular Dichroism (NCD) and Birefringence (NCB), which represent a differential absorption and refraction of circularly polarized light, respectively.[3] Another important manifestation of the light–matter interaction is represented by the Magnetic Optical Activity (MOA), which refers to a differential absorption of circularly polarized light of magnetized matter resulting in the well-known phenomenon of Magnetic Circular Dichroism (MCD).[3–8] Although phenomenologically close, NOA is a consequence of the breaking of inversion symmetry by structural chirality, whereas MOA originates from the breaking of time reversal symmetry by magnetization.[3,4] Moreover, one must keep in mind that both properties are dependent on the state of polarization of light.[3]

There is another optical phenomenon that through the breaking of both time reversal and inversion symmetry allows chiral systems to differentially interact with light when magnetized. This phenomenon can be called Magneto-Chiral Activity (MChA) and manifests itself as a differential absorption or emission of light for Magneto-Chiral Dichroism (MChD) and as anisotropic refraction for Magneto-Chiral Birefringence (MChB).[3,9–11] A key feature of MChA is that it is independent of the state of light polarization. In other words, it can be observed and studied by using unpolarized light sources, which is a practical and technological advantage.

MChD in emission should not be confused with Circularly Polarized Light (CPL) emission. In that case, a chiral system shows emission of CPL upon application of a nonpolarized excitation, even if this phenomenon is now also studied under a magnetic field.[12–14] MChA refers to a modulation of the absorption or emission intensity of light collinear to an applied magnetic field without generation of CPL.

Besides the fascinating aspect of allowing chiral systems to interact with non-chiral unpolarized light, the intensity of

[a]*Univ Rennes, CNRS, ISCR (Institut des Sciences Chimiques de Rennes) – UMR 6226, 35000 Rennes, France. E-mail: fabrice.pointillart@univ-rennes1.fr*
[b]*Laboratoire National des Champs Magnétiques Intenses, CNRS, Univ. Grenoble Alpes, INSA Toulouse, Univ. Toulouse Paul Sabatier, EMFL, 38042 Grenoble, France. E-mail: matteo.atzori@lncmi.cnrs.fr*

MChD responses is proportional to the system magnetization,[11,15,16] making MChD spectroscopy a powerful technique to probe both the optical and magnetic properties of chiral systems.

So far, MChD has been studied in a variety of chemical systems[11,17–20] and metaobjects,[21,22] but most of the studies have been undertaken on chiral complexes containing transition metals[17,18,23–30] and lanthanide ions.[23,31–35] The latter have attracted special attention as a consequence of their high angular momenta and spin–orbit coupling, a prerequisite to observing MChD, resulting in high magnetic anisotropy, as well as the magnetic-dipole allowed characteristic of certain f–f electronic transitions.

In this perspective, we first review the studies on the MChD of chiral lanthanide complexes reported in the literature in both light emission and absorption with light of different wavelengths, and then we provide some general hints that will help the chemical community in designing chiral lanthanide complexes responsive to MChD. Finally, we suggest prospective directions for this emerging and challenging research field.

# Discussion

### Magneto-chiral dichroism in visible light emission

The existence of the magneto-chiral anisotropy and its enantioselectivity were experimentally demonstrated for the first time by G. L. J. A. Rikken and E. Raupach[10] realizing an experiment suggested by G. Wagnière.[36] Tris(3-trifluoroacetyl-±-camphorato)europium(III), Eu((*d*/*l*)tfc)$_3$, complexes (**(*d*/*l*)1-Eu**) were selected as ideal candidates to observe MChD[9] due to the strong natural and magnetic optical activity of $^5D_0 \rightarrow {}^7F_{1,2}$ luminescent transitions.[37–39]

The magneto-chiral luminescence anisotropy was measured for a deuterated DMSO solution of **(*d*/*l*)1-Eu** pair of enantiomers under a 350 nm light irradiation and a 0–0.9 T magnetic field range. The highly luminescent electric-dipole allowed $^5D_0 \rightarrow {}^7F_2$ electronic transitions displayed a weak MChD activity ($g_{MChD}$ = 0.03% at 0.9 T and room temperature) while the weakly luminescent magnetic-dipole allowed $^5D_0 \rightarrow {}^7F_1$ transition displayed a stronger MChD activity ($g_{MChD}$ = 0.12% at 0.9 T and room temperature).

The second study on MChD for visible light emission was published more than 20 years later[19] after the seminal work of Rikken and Raupach. Tb$^{III}$ and Eu$^{III}$ analogues of the compounds $[Ln(L_1^{S,S/R,R})_3](CF_3SO_3)_3$ ($L_1^{S,S/R,R}$ = *S* or *R*-1-(2-naphthyl)ethyl amine, Ln = Tb$^{III}$ (**(*S*,*S*/*R*,*R*)2-Tb**), Eu$^{III}$ (**(*S*,*S*/*R*,*R*)2-Eu**)) (Fig. 1a) and [Ln((*d*/*l*)-tfc)$_3$(phen)] (phen = 1,10-phenanthroline, Ln = Tb$^{III}$ (**(*d*/*l*)3-Tb**)), Eu$^{III}$ (**(*d*/*l*)3-Eu**) (Fig. 1d) were studied.[19] **(*S*,*S*/*R*,*R*)2-Tb** revealed a strong MChD signal for all the $^5D_4 \rightarrow {}^7F_J$ ($J$ = 6, 5, 4, 3) transitions with a maximum value of $g_{MChD}$ = 6% at 1 T and 4.3 K while this value increased to 16% at 14 T and 5 K (Fig. 1b). Similar measurements on the Eu$^{III}$ analogue showed that **(*S*,*S*/*R*,*R*)2-Eu** exhibited a much lower MChD signal for $^5D_0 \rightarrow {}^7F_J$ ($J$ = 1, 2) transitions with a maximum $g_{MChD}$ value of 0.3%. The significant difference in

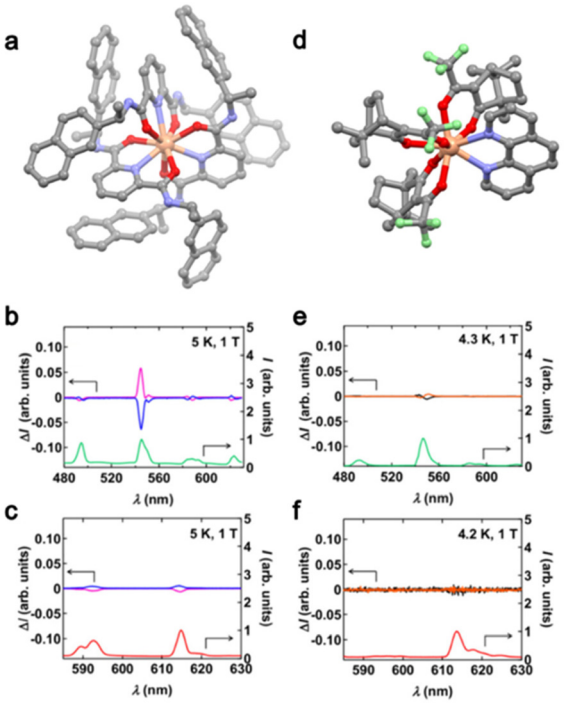


**Fig. 1** (a) Molecular structure of **(*S*,*S*)2-Tb**. Grey, C; red, O; blue, N and salmon, Tb. H atoms and $CF_3SO_3^-$ anions are omitted for clarity. (b) Average luminescence spectrum of **(*S*,*S*)2-Tb** (green line) and MChD spectra of **(*S*,*S*)2-Tb** (pink line) and **(*R*,*R*)2-Tb** (blue line). (c) Average luminescence spectrum of **(*S*,*S*)2-Eu** (red line) and MChD spectra of **(*S*,*S*)2-Eu** (pink line) and **(*R*,*R*)2-Eu** (blue line). (d) Molecular structure of **(*d*)3-Tb**. Grey, C; red, O; blue, N; green, F and salmon, Tb. H atoms are omitted for clarity. (e) Average luminescence spectrum of **(*d*)3-Tb** (green line) and MChD spectra of **(*d*)3-Tb** (black line) and **(*l*)3-Tb** (orange line). (f) Average luminescence spectrum of **(*d*)3-Eu** (red line) and MChD spectra of **(*d*)3-Eu** (black line) and **(*l*)3-Eu** (orange line). Adapted with permission from ref. 12. Copyright 2019, American Physical Society.

MChD activities between the two analogues demonstrated the crucial role of the paramagnetic nature with a large magnetic moment of Tb$^{III}$ ($J$ = 6) compared to the weakly paramagnetic Eu$^{III}$ ($J$ = 0). The first two analogues **(*S*,*S*/*R*,*R*)2-Ln** for which the lanthanide center adopts a symmetrical nona-coordinated geometry were compared with the Tb$^{III}$ and Eu$^{III}$ analogues of **(*d*/*l*)3-Ln**, where the lanthanide adopts a distorted octa-coordinated geometry. The aim was to evaluate the role of the coordination geometry in the MChD response. Under an applied magnetic field of 1 T, **(*d*/*l*)3-Tb** revealed a difference in the luminescence intensity of 1–2% while the MChD signal was almost undetectable for **(*d*/*l*)3-Eu.** For a given lanthanide ion, since the difference in the MChD activity could not be attributed to the difference in magnetization, the authors proposed to attribute it to the difference in coordination sphere, in other words, the degree of the inversion symmetry breaking at the lanthanide site. Such phenomena could be easily evaluated for Eu$^{III}$ using the $R$ ratio between the emission intensities of the electric-dipole allowed transition ($^5D_0 \rightarrow {}^7F_2$) and the magnetic-dipole allowed transition ($^5D_0 \rightarrow {}^7F_1$).[40] The $R$

value is close to 1 for **(*S*,*S*)2-Eu** and 13.6 for **(*d*)3-Eu** leading to a degree of symmetry breaking lower for **(*S*,*S*)2-Eu** than the one for **(*d*)3-Eu**. Moreover, $R$ = 1 is close to the ideal value expected for a strong MChD.[41]

In conclusion, the investigation of K. Taniguchi *et al.* concluded that the MChD signal is ascribed to a combination of strong magnetic moment ($J \neq 0$) and small inversion symmetry breaking at the lanthanide center (high symmetry).

### Magneto-chiral dichroism in hard X-ray absorption

The experimental demonstration of the existence of MChA in emission implies its existence in absorption because of the relationship between Einstein's coefficients in radiative processes.

The motivation to investigate MChD in absorption takes its origin from the fact that large MChD effects are expected for the absorption bands of certain lanthanide complexes.[9] Furthermore, MChD studies on light absorption can provide more quantitative information than those on light emission, which are intrinsically affected by the efficiency of the energy transfer processes, irradiation wavelength, *etc*.

The presence of MChD in the X-ray region (XMChD) was suggested by L. Barron.[3] Indeed, five years after the discovery of the MChD in emission,[10] J. Goulon *et al.*[30] reported the first evidence of X-ray MChD for a magnetoelectric $Cr_2O_3$, and then ten years later, J. R. Galán-Mascarós *et al.* published a study on the observation of MChD in a chiral paramagnetic lanthanide-based complex.[34] In the two investigations, MChD was probed by hard X-ray Absorption Spectroscopy (XAS).

At that time, such spectroscopy was selected because it is element-specific and because one can expect a good signal-to-noise ratio due to the higher extinction coefficients and penetration depths of X-rays than typical UV-vis-NIR absorption experiments.

The XMChD experiments were carried out on the $\{Tb^{III}[Ni^{II}(pro)_2]_6\}^{3+}$ cation (**4**) (pro = (L,D)-prolinate).[42,43] The lanthanide center adopts an icosahedral coordination sphere surrounded by six $Ni^{II}(pro)_2$ units. The first coordination sphere of the $Ni^{II}$ centers formed a perfect octahedra with the (L,D)-prolinate linked at the equatorial positions. The difference between normalized XAS spectra obtained with magnetic field parallel and anti-parallel to the light wavevector led to a non-zero dichroic signal with image mirror when changing from (D)-prolinate to (L)-prolinate. The XMChD reached a maximum value of 1% of the total intensity at the $Tb^{III}$ $L_2$ edge at room temperature and 1 T. Surprisingly, no significant XMChD signal was observed at the $Tb^{III}$ $L_3$ edge even if the theory predicted a stronger dichroic phenomenon at the $L_2$ edge.[44,45] In contrast, the absence of XMChD at the $Ni^{II}$ K-edge was attributed to the weaker spin–orbit coupling and electric quadrupolar contribution for transition metals than for lanthanides. Indeed, it is important to mention here that the electric-dipole/magnetic-dipole characteristic is the key to strong MChD intensity for investigations in the UV-Vis-NIR range while the electric-dipole/electric-quadrupole characteristic is crucial for working with X-rays.

The first attempt to observe XMChD for molecular lanthanide-based complexes was limited to room temperature and low applied magnetic fields (1 T). Therefore, in 2020, S. Piligkos *et al.*[35] reported an experimental observation of XMChD for a mononuclear lanthanide complex formulated as $Na_5[Ho^{III}(ODA)_3](BF_4)_2{\cdot}6H_2O$ (**5-Ho**) ($ODA^{2-}$ = oxydiacetate) (Fig. 2a).[46] $Ho^{III}$ is coordinated to three virtually planar tridentate ODA ligands to form the two *Λ* and *Δ* enantiomers and the nine-coordinated $Ho^{III}$ ion in a distorted face-centered trigonal prismatic coordination sphere ($D_3$). The XMChD experiments were performed at the $L_3$ absorption edge of $Ho^{III}$ because the promotion of a 2p core electron into an empty 5d or 6s valence state *via* the electric-dipole allowed transition ($\Delta l$ = ±1) and 2p into a 6p or 4f state ($\Delta l$ = 0, +2) *via* electric-quadrupole transitions can be easily disentangled at the lanthanide $L_3$-edge,[47] while their contributions at the $L_2$-edge is more difficult to disentangle.[48] A XMChD signal of opposite sign for **(*Λ*)5-Ho** and **(*Δ*)5-Ho** was observed at the pre-edge (8069 eV) and the main (8078 eV) absorptions, but not in the extended region (Fig. 2b).[35] Such observations confirmed that non-magnetic empty 6p and 6d states did not contribute to the XMChD signal while 4f and 5d did because of their orbital angular momentum contribution. The maximum XMChD activity was evaluated at 0.05% at 2.7 K under an applied magnetic field of 4 T. The authors attributed the weak XMChD activity of **(*Λ*/*Δ*)5-Ho** compared to **(L/D)-4** to the strong localization of the 4f orbitals and weak hybridization with the 5d orbitals. Nevertheless, the difference in the lanthanide ion, local coordination symmetry and probed edge makes a direct comparison between the XMChD activities of these two compounds difficult.

### Magneto-chiral dichroism in visible light absorption

From the previous works, one can draw a few conclusions. It appears that the (X)MChD strongly depends on the angular moments of the lanthanide ($L$ and $J \neq 0$), the spin–orbit coupling and the symmetry of the coordination sphere (degree of inversion symmetry breaking). All these parameters are driven by the nature of the lanthanide and the crystal field in the complex leading to the magnetic anisotropy, which is indeed a key parameter in molecular magnetism to design Single-

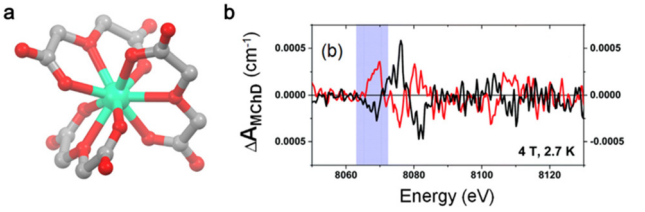


**Fig. 2** (a) Molecular structure of **5-Ho**, $Na^+$ cations, and $BF_4^-$ anions; hydrogen atoms and water molecules of crystallization were omitted for clarity. Grey, C; red, O and green, Ho. (b) XMChD signal recorded for Λ (red line) and Δ (black line) at the Ho $L_3$-edge at 2.7 K with an applied magnetic field of 4 T. The blueish zone corresponds to the pre-edge absorption. Adapted with permission from ref. 27. Copyright 2020, Royal Society of Chemistry.

Molecule Magnets (SMMs). Thus, together with our colleagues, we decided to study both magnetic and (chiro)optical properties of enantiopure ytterbium(III) helicene-based compounds.[23]

The helicoidal chirality of helicene comes from the *ortho*-fused (hetero) aromatic rings with extended π-conjugation, and they are well-known to display remarkable chiroptical activity.[49–52] $Yb^{III}$ has been selected because it has one of the simplest electronic configurations among the lanthanide series with only one excited multiplet ($^2F_{5/2}$) leading to a unique magnetic-dipole allowed ($|\Delta J| = 1$) electronic transition ($^2F_{7/2} \rightarrow {}^2F_{5/2}$).

First, the pair of enantiomers formulated as [Yb($L_2^{(P,M)}$)(hfac)$_3$] ($L_2$ = 3-(2-pyridyl)-4-aza[6]-helicene; $hfac^-$ = 1,1,1,5,5,5-hexafluoroacetylacetonate) (**(*P*/*M*)6-Yb**) was prepared as single crystals.[31,53,54] The crystal structure revealed mononuclear complexes in which $Yb^{III}$ is surrounded by six oxygen atoms coming from three $hfac^-$ ancillary anions and two nitrogen atoms coming from the $L_2^{(P/M)}$ ligand (Fig. 3a). A distorted $D_{2d}$ coordination sphere was identified and a *Δ* and *Λ* lanthanide-centered chirality driven by the $L_2^{(P)}$ and $L_2^{(M)}$ ligands, respectively, was observed. The direct current magnetic susceptibility measurements revealed a $\chi_M T$ value of 2.24 $cm^3\ K\ mol^{-1}$ at room temperature and a magnetization of $1.73N\beta$ at 5 T in agreement with an $Yb^{III}$ ($S = \frac{1}{2}$, $L = 3$ and $g_J = 8/7$). The alternating current susceptibility measurements highlighted a slow magnetic relaxation at 2 K and 1 kOe, revealing a significant magnetic anisotropy. Both enantiomers of **6-Yb** showed the usual NIR $Yb^{III}$ centered luminescence at 77 K with additional bands due to hot bands and vibronic contributions. A combination of both chirality and emission opens the possibility to investigate their cross effects called Circularly Polarized Luminescence (CPL). Solid-state irradiation at 365 nm induced a strong mirror image CPL signal for **(*P*/*M*)6-Yb** with a maximum $g_{lum}$ factor of 0.13 at 977 nm (Fig. 3b).[33] By measuring the absorption spectra at 4 K on an oriented single crystal perpendicular to the [011] crystallographic face, it was possible to determine the energy splitting of the excited $^2F_{5/2}$ multiplet. The complete experimental energy level diagram for both the $^2F_{7/2}$ ground multiplet and the $^2F_{5/2}$ excited multiplet under the crystal field effect was rationalized by *ab initio* calculations.

These studies demonstrated that the helical ligands provided a strong-enough chiral environment around the $Yb^{III}$ center for MChD investigation.

Accordingly, the first experimental MChD measurements through visible-NIR light absorption were carried out at 4 K in the 0–1.68 T magnetic field range, allowing the observation of a fine-structured strong MChD signal associated with the $^2F_{7/2} \rightarrow {}^2F_{5/2}$ transition (Fig. 3c). The asymmetric factor $g_{MChD}$ was evaluated at 0.12% at 0.86 T and 4 K, which is in the same order of magnitude as that of **(*S*,*S*/*R*,*R*)2-Tb** (0.06% at 1 T and 4.3 K) determined by light emission. The MChD signal is strong enough to perform a temperature dependence study in the 4–150 K temperature range (Fig. 3d). Both field (Fig. 3c) and thermal (Fig. 3d) dependences of the MChD signal were

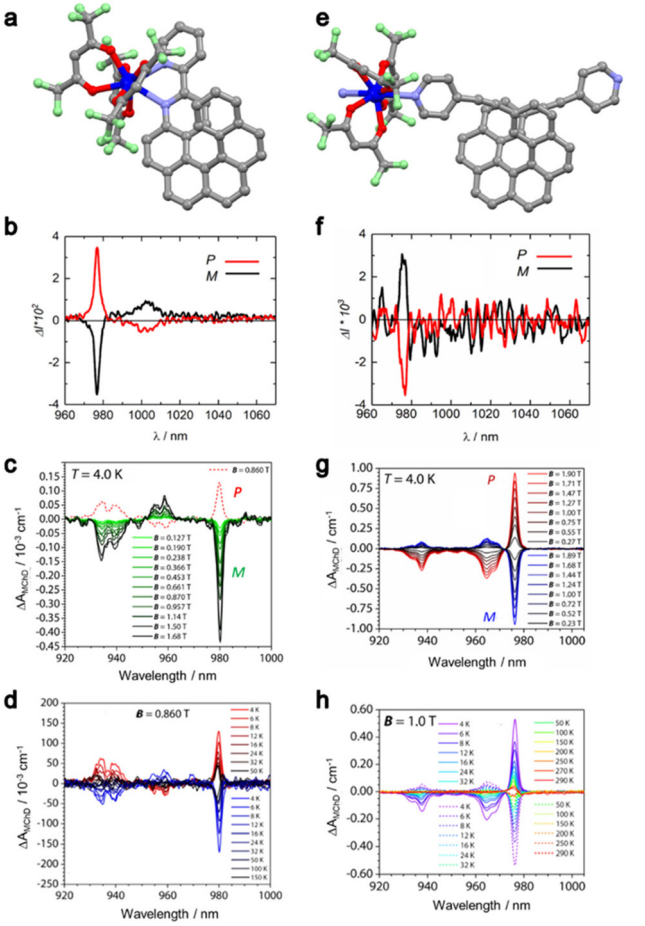


**Fig. 3** Molecular structure of **(*P*)6-Yb** (a) and **[(*P*)7-Yb]$_n$** (e); H atoms and solvent molecules of crystallization were omitted for clarity. Grey, C; red, O; blue, N and dark blue, Yb. CPL spectra (at 298 K) of **(*P*)6-Yb** (red line)/**(*M*)6-Yb** (black line) (b) and **[(*P*)7-Yb]$_n$** (red line)/**[(*M*)7-Yb]$_n$** (black line) (f) under 365 nm excitation in solid-state. Field dependence of the difference in the absorption $\Delta A_{MChD}$ of the $^2F_{7/2} \rightarrow {}^2F_{5/2}$ transition at 4 K for **(*P*/*M*)6-Yb** (c) and **[(*P*/*M*)7-Yb]$_n$** (g). Thermal dependence of the difference in the absorption $\Delta A_{MChD}$ of the $^2F_{7/2} \rightarrow {}^2F_{5/2}$ transition for **(*P*/*M*)6-Yb** under 0.86 T (d) and **[(*P*/*M*)7-Yb]$_n$** under 1 T (h). Adapted with permission from ref. 23 and 25. Copyright 2021, American Chemical Society. Copyright 2023, Wiley-VCH Verlag GmbH & Co. KGaA Weinheim.

compared to the thermal and field dependences of the magnetization determined by magnetometry with a perfect agreement. The thermal dependence of the MChD signal allowed us to verify the Barron and Vrbancich microscopic theory of MChD formulated on the basis of the Magnetic Circular Dichroism (MCD) theory. At low temperatures ($T < 15$ K), the so-called MChD *C* term (analogous to the Faraday *C* term in MCD), which is temperature dependent due to a variation of the population of the ground state and associated with an absorptive line-shape, dominates. For $T > 20$ K, the so-called MChD *A* term (analogous to the Faraday *A* term in MCD), which is due to the Zeeman energy splitting and hence temperature independent and associated with a derivative-type line-shape, dominates.

A similar magnetic and chiroptical investigation was carried out on a second pair of enantiomers using the 2,15-bis-(4-pyridyl)-ethynyl-carbo[6]helicene ($L_3^{(P/M)}$) ligand instead of $L_2^{(P/M)}$. The reaction of $L_3^{(P/M)}$ with the $Yb(hfac)_3(H_2O)_2$ metallic precursor led to the formation of enantiopure coordination polymers of the formula $[L_3^{(P/M)}Yb(hfac)_3]_n$ (**[(*P*/*M*)7-Yb]$_n$**).[33] A slightly distorted $D_{2d}$ $N_2O_6$ surrounding is found around the $Yb^{III}$ centers as found for the mononuclear complexes **(*P*/*M*)6-Yb**.

From a magnetic point of view, the main difference comes from the clear SMM behavior observed under an applied magnetic field of 1600 Oe with a magnetic relaxation occurring through a combination of Orbach and Raman processes. Such an enhancement of magnetic performances could be rationalized by the "*trans*" position of the nitrogen atoms in **[(*P*/*M*)7-Yb]$_n$** while they have been observed in the "*cis*" position in **(*P*/*M*)6-Yb** leading to a smaller electronic repulsion for the prolate $Yb^{III}$ ion, *i.e.* a stronger spin–orbit coupling/axial magnetic anisotropy in the polymeric structures. Such qualitative analysis was confirmed by *ab initio* calculations which concluded that the ground Kramers doublet is mainly composed of $M_J = \pm 5/2$ ($g_z = 4.0$) for **(*P*/*M*)6-Yb** and $M_J = \pm 7/2$ ($g_z = 7.0$) for **[(*P*/*M*)7-Yb]$_n$**.

Irradiation at 365 nm of **[(*P*/*M*)7-Yb]$_n$** led to a strong NIR emission of the $Yb^{III}$ center with the total energy splitting similar to the one observed for the mononuclear systems but with a different shape (relative intensity and energy position of the emission lines) which is in agreement with a similar crystal field but different electronic distributions for both monomeric and polymeric systems. Attempts to measure CPL at room temperature in the solid state led to the observation of a weak mirror image signal for both enantiomers of **[(*P*/*M*)7-Yb]$_n$** with a maximum dissymmetry factor $g_{lum}$ of 0.007 at 978 nm (Fig. 3f). One could deduce from the CPL spectra that only a weak chiral environment is present around $Yb^{III}$ in **[(*P*/*M*)7-Yb]$_n$**. In contrast, MChD measurements performed on single crystals of **[(*P*/*M*)7-Yb]$_n$** at 4 K in the 0–1.90 T magnetic field revealed a remarkably high MChD signal (Fig. 3g) with $g_{MChD} = 0.19\ T^{-1}$ at 1 T and 4 K. Such a value is the highest reported value for lanthanide complexes. The MChD activity was strong enough to observe a differential absorption $\Delta A_{MChD}$ up to room temperature under an applied magnetic field of 1 T (Fig. 3h). In conclusion, despite the weaker chiral environment in **[(*P*/*M*)7-Yb]$_n$** compared to **(*P*/*M*)6-Yb**, a stronger MChD activity was measured due to the stronger magnetic anisotropy determined by both magnetometry and *ab initio* calculations.

MChD measurements through light absorption were also performed for the heterobimetallic 3d–4f complexes of the formula $[Ln_5Ni_6((R/S)\text{-}HL_4)_6(Ac)_3(\mu_3\text{-}OH)_9(H_2O)_6](ClO_4)_3(H_2O)_{15}$ ($H_3L_3$ = (*R*/*S*)-(2-hydroxy-3-methoxybenzyl)-serine, Ln = $Dy^{III}$ **(*R*/*S*)8-DyNi**, $Y^{III}$ **(*R*/*S*)8-YNi**).[23] The room temperature NCD of both $Dy^{III}$ and $Y^{III}$ analogues displayed two components at 670 nm and 1190 nm (Fig. 4a) which are associated with the $^3T_1/^3T_2/^3A_1/^3E \leftarrow {}^3A_2$ transitions of the octahedral $Ni^{II}$.[28,55,56] Since both NCD spectra are identical, one could conclude that the electronic transitions for $Dy^{III}$ do not contribute to the NCD. In contrast, the MCD spectra for **(*R*/*S*)8-DyNi** are composed of two weak and broad contributions of $Ni^{II}$ and a series of intense and sharp signals associated with $Dy^{III}$ (Fig. 4c). Deep analysis of the MCD spectra of **(*R*/*S*)8-DyNi** highlighted a splitting of the MCD contributions, which has been attributed to the presence of the two crystallographically independent $Dy^{III}$ centers. The thermal dependence of the MChD was measured at 0.86 T in the 4–150 K temperature range (Fig. 4d). It displayed contributions coming from both the $Ni^{II}$ and the $Dy^{III}$ centers, in contrast with what was observed in XMChD for the heterobimetallic complex **4**.[34]

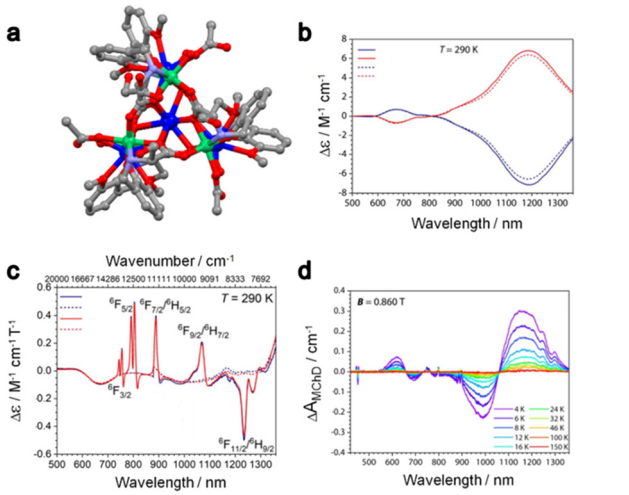


**Fig. 4** (a) Molecular structure of **(*R*/*S*)8-DyNi**; H atoms, $ClO_4^-$ anions and solvent molecules of crystallization were omitted for clarity. Grey, C; red, O; blue, Dy and green, Ni. (b) Room temperature NCD spectra of **(*R*)8-DyNi** (blue line), **(*S*)8-DyNi** (red line), **(*R*)8-YNi** (dashed blue line) and **(*S*)8-YNi** (dashed red line) in MeOH solution. (c) Room temperature MCD spectra of **(*R*)8-DyNi** (blue line), **(*S*)8-DyNi** (red line), **(*R*)8-YNi** (dashed blue line) and **(*S*)8-YNi** (dashed red line) in MeOH solution. (d) Thermal variation of MChD spectra of **(*R*)8-DyNi** recorded on an oriented single crystal under an applied field of 0.86 T. Adapted with permission from ref. 16. Copyright 2022, American Chemical Society.

Focusing on the MChD contributions of the $Dy^{III}$ centers, the two $Dy^{III}$ sites did not provide MChD signals of the same intensity. The most intense $Dy^{III}$ MChD signals were attributed to the three $Dy^{III}$ ions that occupy the external position of the clusters. Such attribution is in agreement with the fact that such eight-coordinated $Dy^{III}$ ions are closer to the chiral ligand than the two nine-coordinated $Dy^{III}$ ions, although the difference in the magnetic anisotropy between the two $Dy^{III}$ ions cannot be ruled out at this stage. In conclusion, the authors associated the $Ni^{II}$ MChD as mainly driven by its NOA while the MChD of $Dy^{III}$ as mainly driven by its MOA.

Together with the magnetic and chiroptical investigations performed on **(*P*/*M*)6-Yb** and **[(*P*/*M*)7-Yb]$_n$**, underlining that the magnetic anisotropy of the ground state was the leading factor of MChD in these species, this study confirms that engineering the magnetic anisotropy of the Ln systems is a more efficient strategy than optimizing the chirality at the metal center to enhance the MChD response in lanthanide systems. At the same time, although it is not the focus of this

perspective, this result also highlights that the reverse is true for transition metal ions, confirming the observations performed on chiral Prussian blue analogues.[24,25]

Testing the potential use of MChD as a tool for the optical readout of the magnetic states without the need for light polarization motivated us to investigate the MChD properties of the $Dy^{III}$ analogue of **[(*P*/*M*)7-Ln]$_n$**. The $Dy^{III}$ ion is undoubtedly the most used lanthanide ion for designing SMMs due to its high magnetic moment and strong magnetic anisotropy. Magnetic field dependent MChD signals for **[(*P*/*M*)7-Dy]$_n$** were observed for each electronic transition detected in absorption at 4 K, *i.e.* $^6F_{n/2}/^6H_{m/2} \leftarrow {}^6H_{15/2}$ transitions with $n$ = 3, 5, 7, 9 and 11 and $m$ = 5, 7 and 9.[32] The maximum $g_{MChD}$ factor was determined to be equal to 1.2% at 1 T and 4 K, which is one order of magnitude lower than that observed for the $Yb^{III}$ analogue. This difference can be rationalized on the basis of the nature of the investigated electronic transitions. Those of **[(*P*/*M*)7-Dy]$_n$** are magnetic-dipole forbidden and only induced electric-dipole allowed, while for **[(*P*/*M*)7-Yb]$_n$** the unique displayed transition is magnetic-dipole allowed.[57,58] Although weak, the MChD activity for **[(*P*/*M*)7-Dy]$_n$** was observed for all the electronic transitions up to 32 K under 1 T, which makes chiral $Dy^{III}$-based SMMs good candidates to demonstrate the optical readout of magnetic states with unpolarized light.

## Concluding remarks and perspectives

As examined in this perspective, chiral lanthanide complexes, which inherently show high spin–orbit coupling, a variety of electronic configurations, a multitude of electronic transitions of different characteristics, variable coordination geometries and different degrees of magnetic anisotropy, represent ideal molecules to investigate MChD in both light absorption and emission in a wide spectral range (from near-infrared to hard X-rays). Although only a limited number of studies have been undertaken so far, one can summarize some general findings that can help the chemical community in designing chiral lanthanide complexes responsive to MChD.

1. For lanthanide complexes, it seems that a short distance between the chiral and the magnetic centers is not crucial to observe strong MChD responses. In turn, the leading parameter for intense MChD appears to be related to the electronic, thus magnetic, configuration of the ground state of the lanthanide center and not the chiral features of the coordination sphere. This was deduced from theoretical calculations as well as from experimental evidence such as the temperature dependence of the MChD signals and the determinant influence of the MCD intensity on the MChD one. To definitely establish this, NCD, MCD and MChD measurements have to be performed on the same sample and under the very same conditions of orientation, temperature and magnetic field (for MCD and MChD). It is challenging, from an instrumental point of view, to perform measurements at low temperatures under a magnetic field with polarized light. The complexity of the experiment is further increased by the linear birefringence shown by single crystals all the more since these effects can be more intense than those related to NOA and MOA and hinder quantitative determination. Indeed, most NCD and MCD studies at low temperature are performed on frozen solutions.

2. The higher the magnetic anisotropy, the higher the MChD response, with important differences in intensity expected if the probed orientation (wavevector and magnetic field) is along the magnetic anisotropy easy axis or perpendicular to it. This can be deduced by the similarity of the MChD response of lanthanide complexes with respect to the MCD theory, which also defines the angular dependency of the MCD response with respect to the anisotropy of the *g*-factor. This has not been experimentally demonstrated so far, but it can constitute a remarkable advancement to corroborate the MChD microscopic theory.

3. From a coordination chemistry point of view, one can consider that all the structural and electronic design criteria identified to develop SMMs with a high blocking temperature and energy barriers also apply to maximize MChD responses. The chemical challenge is to introduce chirality into the ligands while keeping the same structural and electronic parameters. It should be noted that chirality has been introduced in some SMMs to improve the energy barrier and/or to limit the relaxation pathways, but with no real interest in the optical enantiopurity of the resulting compounds, which is instead crucial for MChD.

4. The characteristics of the electronic transition have a crucial importance in determining the intensity of the MChD signals, regardless of the chirality of the ligands, the distortion of the coordination geometry and the magnetic anisotropy of the investigated systems: magnetic-dipole allowed transitions overall provide higher responses with respect to electric-dipole allowed as far as the visible-NIR range is concerned. Nonetheless, for a given lanthanide ion and a given electronic transition, the optimization of the above-mentioned parameters can be used to further maximize the MChD intensity.

Several experiments and studies are still needed to clearly elucidate this fascinating phenomenon and to fully understand how to maximize the MChD intensity for practical applications.

1. It can be clearly seen that the number of studies on MChD with light emission is very limited with respect to those with absorption. The fascinating properties of chiral lanthanide complexes as circularly polarized light emitters motivate further studies in this direction for comparing both the CPL and MChD properties in emission, including CPL under a magnetic field, and also the MChD properties in absorption and emission for the same system. With the same mindset, one can envisage MChD studies on the same system with light sources of very different energies, such as visible light and X-rays or visible light and microwaves. This will provide a better view of the microscopic parameters that have to be implemented and optimized as a function of the electronic transition and, from an application point of view, the light energy of interest.

2. So far, although extremely challenging, *ab initio* theoretical calculations of MChD have been reported only for a $Ni^{II}$-

 

based complex with a relatively simple electronic configuration.[28] The implementation of MChD theoretical calculations on lanthanide complexes, although more challenging as a consequence of their electronic properties and configurations with respect to those of transition metal ions, is expected to provide a substantial contribution to chemical design and experiment rationalization.

3. One can also envision to switch on and off the MChD properties by using chiral switchable ligands responsive to external stimuli (temperature, light, redox processes, electric field, *etc*.) and able to modify the coordination geometry around the lanthanide center or activate/deactivate the chiral influence of the ligand towards the lanthanide center.

4. Finally, as recently proposed but not experimentally demonstrated yet, MChD can be used to read out the magnetic state of SMMs by means of unpolarized light. This can be realized on chiral SMMs or chiral ferromagnets having an opened hysteresis cycle at a temperature viable for MChD measurements with an adapted measurement protocol able to follow the system magnetization dynamics. This extremely challenging demonstration will represent a breakthrough in the field of optical readout of magnetic data because novel polarization-free optical data readout technologies can result from this demonstration, contrary to current technologies.

## Conflicts of interest

There are no conflicts to declare.

## Acknowledgements

The French National Research Agency (ANR) is acknowledged for the financial support through the SWITCH-MChD (ANR-23-CE07-0003) and MaChiNaCo (ANR-19-CE09-0018) projects.

## References

1 G. H. Wagnière, *On Chirality and the Universal Asymmetry*, Wiley, Weinheim, Germany, 2007.
2 M. Yus and A. Guijarro, *The Origin of Chirality in the Molecules of Life*, Royal Society of Chemistry, Cambridge, 2008.
3 L. D. Barron, *Molecular Light Scattering and Optical Activity*, Cambridge University Press, 2004.
4 P. J. Stephens, Theory of Magnetic Circular Dichroism, *J. Chem. Phys.*, 1970, **52**, 3489.
5 P. Comba, L. J. Daumann, R. Klingeler, C. Koo, M. J. Riley, A. E. Roberts, H. Wadepohl and J. Werner, Correlation of Structural and Magnetic Properties in a Set of Mononuclear Lanthanide Complexes, *Chem. – Eur. J.*, 2018, **24**, 5319–5330.
6 J. Mack, M. J. Stillman and N. Kobayashi, Application of MCD spectroscopy to porphyrinoids, *Coord. Chem. Rev.*, 2007, **251**, 429–453.
7 W. R. Mason, *A Practical Guide to Magnetic Circular Dichroism Spectroscopy*, John Wiley & Sons, Inc., Hoboken, NJ, USA, 2007.
8 Y. Kitagawa, S. Wada, K. Yanagisawa, T. Nakanishi, K. Fushimi and Y. Hasegawa, Molecular Design Guidelines for Large Magnetic Circular Dichroism Intensities in Lanthanide Complexes, *ChemPhysChem*, 2016, **17**, 845–849.
9 L. D. Barron and J. Vrbancich, Magneto-chiral birefringence and dichroism, *Mol. Phys.*, 1984, **51**, 715–730.
10 G. L. J. A. Rikken and E. Raupach, Observation of magneto-chiral dichroism, *Nature*, 1997, **390**, 493–494.
11 M. Atzori, G. L. J. A. Rikken and C. Train, Magneto–Chiral Dichroism: A Playground for Molecular Chemists, *Chem. – Eur. J.*, 2020, **26**, 9784–9791.
12 F. Zinna and L. Di Bari, Lanthanide Circularly Polarized Luminescence: Bases and Applications, *Chirality*, 2015, **27**, 1–13.
13 O. G. Willis, F. Zinna and L. Di Bari, NIR–Circularly Polarized Luminescence from Chiral Complexes of Lanthanides and d–Metals, *Angew. Chem., Int. Ed.*, 2023, **62**, e202302358.
14 F. Zinna and G. Pescitelli, Magnetic Circularly Polarized Luminescence of Organic Compounds, *Eur. J. Org. Chem.*, 2023, **26**, e202300509.
15 C. Train, R. Gheorghe, V. Krstic, L.-M. Chamoreau, N. S. Ovanesyan, G. L. J. A. Rikken, M. Gruselle and M. Verdaguer, Strong magneto-chiral dichroism in enantiopure chiral ferromagnets, *Nat. Mater.*, 2008, **7**, 729–734.
16 M. Atzori, C. Train, E. A. Hillard, N. Avarvari and G. L. J. A. Rikken, Magneto–chiral anisotropy: From fundamentals to perspectives, *Chirality*, 2021, **33**, 844–857.
17 R. Sessoli, M.-E. Boulon, A. Caneschi, M. Mannini, L. Poggini, F. Wilhelm and A. Rogalev, Strong magneto-chiral dichroism in a paramagnetic molecular helix observed by hard X-rays, *Nat. Phys.*, 2015, **11**, 69–74.
18 K. Taniguchi, S. Kishiue, S. Kimura and H. Miyasaka, Local-Site Dependency of Magneto-Chiral Dichroism in Enantiopure One-Dimensional Copper(II)–Chromium(III) Coordination Polymers, *J. Phys. Soc. Jpn.*, 2019, **88**, 93708.
19 K. Taniguchi, M. Nishio, S. Kishiue, P.-J. Huang, S. Kimura and H. Miyasaka, Strong magnetochiral dichroism for visible light emission in a rationally designed paramagnetic enantiopure molecule, *Phys. Rev. Mater.*, 2019, **3**, 45202.
20 Y. Kitagawa, H. Segawa and K. Ishii, Magneto-Chiral Dichroism of Organic Compounds, *Angew. Chem., Int. Ed.*, 2011, **50**, 9133–9136.
21 S. Tomita, K. Sawada, A. Porokhnyuk and T. Ueda, Direct Observation of Magnetochiral Effects through a Single Metamolecule in Microwave Regions, *Phys. Rev. Lett.*, 2014, **113**, 235501.
22 S. Tomita, K. Sawada, H. Kurosawa and T. Ueda, in *Springer Series in Materials Science*, 2019.
23 X. Wang, S.-Q. Wang, J.-N. Chen, J.-H. Jia, C. Wang, K. Paillot, I. Breslavetz, L.-S. Long, L. Zheng, G. L. J. A. Rikken, C. Train, X.-J. Kong and M. Atzori,

Magnetic 3d–4f Chiral Clusters Showing Multimetal Site Magneto-Chiral Dichroism, *J. Am. Chem. Soc.*, 2022, **144**, 8837–8847.

24 M. Atzori, I. Breslavetz, K. Paillot, K. Inoue, G. L. J. A. Rikken and C. Train, A Chiral Prussian Blue Analogue Pushes Magneto-Chiral Dichroism Limits, *J. Am. Chem. Soc.*, 2019, **141**, 20022–20025.

25 M. Atzori, I. Breslavetz, K. Paillot, G. L. J. A. Rikken and C. Train, Role of structural dimensionality in the magneto-chiral dichroism of chiral molecular ferrimagnets, *J. Mater. Chem. C*, 2022, **10**, 13939–13945.

26 N. Nakagawa, N. Abe, S. Toyoda, S. Kimura, J. Zaccaro, I. Gautier-Luneau, D. Luneau, Y. Kousaka, A. Sera, M. Sera, K. Inoue, J. Akimitsu, Y. Tokunaga and T. Arima, Magneto-chiral dichroism of CsCuCl3, *Phys. Rev. B*, 2017, **96**, 121102.

27 B. Sun, X.-F. Liu, X.-Y. Li, Y. Zhang, X. Shao, D. Yang and H.-L. Zhang, Two-Dimensional Perovskite Chiral Ferromagnets, *Chem. Mater.*, 2020, **32**, 8914–8920.

28 M. Atzori, H. Ludowieg, M. Cortijo, I. Breslavetz, K. Paillot, P. Rosa, C. Train, J. Autschbach, E. A. Hillard and G. L. J. A. Rikken, Validation of Microscopic Magneto-Chiral Dichroism Theory, *Sci. Adv.*, 2021, **7**, eabg2859.

29 M. Atzori, F. Santanni, I. Breslavetz, K. Paillot, A. Caneschi, G. L. J. A. Rikken, R. Sessoli and C. Train, Magnetic Anisotropy Drives Magnetochiral Dichroism in a Chiral Molecular Helix Probed with Visible Light, *J. Am. Chem. Soc.*, 2020, **142**, 13908–13916.

30 J. Goulon, A. Rogalev, F. Wilhelm, C. Goulon-Ginet, P. Carra, D. Cabaret and C. Brouder, X-Ray Magnetochiral Dichroism: A New Spectroscopic Probe of Parity Nonconserving Magnetic Solids, *Phys. Rev. Lett.*, 2002, **88**, 237401.

31 M. Atzori, K. Dhbaibi, H. Douib, M. Grasser, V. Dorcet, I. Breslavetz, K. Paillot, O. Cador, G. L. J. A. Rikken, B. Le Guennic, J. Crassous, F. Pointillart and C. Train, Helicene-Based Ligands Enable Strong Magneto-Chiral Dichroism in a Chiral Ytterbium Complex, *J. Am. Chem. Soc.*, 2021, **143**, 2671–2675.

32 M. S. Raju, K. Dhbaibi, M. Grasser, V. Dorcet, I. Breslavetz, K. Paillot, N. Vanthuyne, O. Cador, G. L. J. A. Rikken, B. Le Guennic, J. Crassous, F. Pointillart, C. Train and M. Atzori, Magneto-Chiral Dichroism in a One-Dimensional Assembly of Helical Dysprosium(III) Single-Molecule Magnets, *Inorg. Chem.*, 2023, **62**, 17583–17587.

33 K. Dhbaibi, M. Grasser, H. Douib, V. Dorcet, O. Cador, N. Vanthuyne, F. Riobé, O. Maury, S. Guy, A. Bensalah-Ledoux, B. Baguenard, G. L. J. A. Rikken, C. Train, B. Le Guennic, M. Atzori, F. Pointillart and J. Crassous, Multifunctional Helicene–Based Ytterbium Coordination Polymer Displaying Circularly Polarized Luminescence, Slow Magnetic Relaxation and Room Temperature Magneto–Chiral Dichroism, *Angew. Chem.*, 2023, **135**, e202215558.

34 M. Ceolín, S. Goberna-Ferrón and J. R. Galán-Mascarós, Strong Hard X-ray Magnetochiral Dichroism in Paramagnetic Enantiopure Molecules, *Adv. Mater.*, 2012, **24**, 3120–3123.

35 D. Mitcov, M. Platunov, C. D. Buch, A. Reinholdt, A. R. Døssing, F. Wilhelm, A. Rogalev and S. Piligkos, Hard X-ray magnetochiral dichroism in a paramagnetic molecular 4f complex, *Chem. Sci.*, 2020, **11**, 8306–8311.

36 G. Wagnière, Magnetochiral dichroism in emission. Photoselection and the polarization of transitions, *Chem. Phys. Lett.*, 1984, **110**, 546–551.

37 H. G. Brittain and F. S. Richardson, Circularly polarized emission studies on the chiral nuclear magnetic resonance lanthanide shift reagent tris(3-trifluoroacetyl-d-camphorato) europium(III), *J. Am. Chem. Soc.*, 1976, **98**, 5858–5863.

38 P. H. Schippers, A. van den Buekel and H. P. J. M. Dekkers, An accurate digital instrument for the measurement of circular polarisation of luminescence, *J. Phys. E: Sci. Instrum.*, 1982, **15**, 945–945.

39 C. Görller-Walrand and J. Godemont, MCD of the $Eu^{3+}$ ion in aqueous solution. Analysis of the $^5D_{,0,1,2} \leftarrow {}^7F_{0,1,2}$ transitions, *J. Chem. Phys.*, 1977, **67**, 3655–3658.

40 Y. Hasegawa, M. Yamamuro, Y. Wada, N. Kanehisa, Y. Kai and S. Yanagida, Luminescent Polymer Containing the Eu (III) Complex Having Fast Radiation Rate and High Emission Quantum Efficiency, *J. Phys. Chem. A*, 2003, **107**, 1697–1702.

41 Y. Tokura and N. Nagaosa, Nonreciprocal responses from non-centrosymmetric quantum materials, *Nat. Commun.*, 2018, **9**, 3740.

42 Y. Yukawa, S. Igarashi, A. Yamano and S. Sato, Structure of the centred icosahedral samarium cluster formed by bis(l-prolinato)nickel(II) ligands, *Chem. Commun.*, 1997, 711–712.

43 Y. Yukawa, G. Aromí, S. Igarashi, J. Ribas, S. A. Zvyagin and J. Krzystek, [$GdNi_6$] and [$LaNi_6$]: High–Field EPR Spectroscopy and Magnetic Studies of Exchange–Coupled Octahedral Clusters, *Angew. Chem., Int. Ed.*, 2005, **44**, 1997–2001.

44 K. Fukui, H. Ogasawara, A. Kotani, I. Harada, H. Maruyama, N. Kawamura, K. Kobayashi, J. Chaboy and A. Marcelli, X-ray magnetic circular dichroism at rare-earth $L_{2,3}$ edges in $R_2Fe_{14}B$ compounds (R = La, Pr, Nd, Sm, Gd, Tb, Dy, Ho, Er, Tm, Yb, and Lu), *Phys. Rev. B: Condens. Matter Mater. Phys.*, 2001, **64**, 104405.

45 M. Nakazawa, K. Fukui and A. Kotani, Theory of X-ray absorption and resonant X-ray emission spectra by electric quadrupole excitation in light rare-earth systems, *J. Solid State Chem.*, 2003, **171**, 295–298.

46 C. Kremer, J. Torres and S. Domínguez, Lanthanide complexes with oda, ida, and nta: From discrete coordination compounds to supramolecular assemblies, *J. Mol. Struct.*, 2008, **879**, 130–149.

47 C. Dallera, M. Krisch, A. Rogalev, J. Goulon and F. Sette, Resonant inelastic X-ray scattering at the $L_3$ edge of $Eu^{2+}$, $Gd^{3+}$, and $Tb^{4+}$ compounds, *Phys. B*, 2002, **312–313**, 850–852.

48 M. Platunov, N. Kazak, V. Dudnikov, V. Temerov, I. Gudim, Y. Knyazev, S. Gavrilkin, V. Dyadkin, I. Dovgaliuk,

 

D. Chernyshov, A. Hen, F. Wilhelm, A. Rogalev and S. Ovchinnikov, Element selective magnetism in $Ho_{0.5}Nd_{0.5}Fe_3(BO_3)_4$ single crystal probed with hard X-ray magnetic circular dichroism, *J. Magn. Magn. Mater.*, 2019, **479**, 312–316.

49 C.-F. Chen and Y. Shen, *Helicene Chemistry*, Springer Berlin Heidelberg, Berlin, Heidelberg, 2017.

50 K. Dhbaibi, L. Favereau and J. Crassous, Enantioenriched Helicenes and Helicenoids Containing Main-Group Elements (B, Si, N, P), *Chem. Rev.*, 2019, **119**, 8846–8953.

51 M. Gingras, G. Félix and R. Peresutti, One hundred years of helicene chemistry. Part 2: stereoselective syntheses and chiral separations of carbohelicenes, *Chem. Soc. Rev.*, 2013, **42**, 1007–1050.

52 J. Crassous, I. G. Stará and I. Starý, *Helicenes – Synthesis, Properties and Applications*, Wiley, 2022.

53 J.-K. Ou-Yang, N. Saleh, G. Fernandez Garcia, L. Norel, F. Pointillart, T. Guizouarn, O. Cador, F. Totti, L. Ouahab, J. Crassous and B. Le Guennic, Improved slow magnetic relaxation in optically pure helicene-based $Dy^{III}$ single molecule magnets, *Chem. Commun.*, 2016, **52**, 14474–14477.

54 M. Galland, F. Riobé, J. Ouyang, N. Saleh, F. Pointillart, V. Dorcet, B. Le Guennic, O. Cador, J. Crassous, C. Andraud, C. Monnereau and O. Maury, Helicenic Complexes of Lanthanides: Influence of the f–Element on the Intersystem Crossing Efficiency and Competition between Luminescence and Oxygen Sensitization, *Eur. J. Inorg. Chem.*, 2019, **2019**, 118–125.

55 M. C. L. Yang and R. A. Palmer, Natural solid state optical activity of tris(ethylenediamine)metal(II) nitrates. II. Single-crystal circular and linear dichroism spectra of tris(ethylenediamine)cobalt(II) nitrate, *J. Am. Chem. Soc.*, 1975, **97**, 5390–5395.

56 M. C.-L. Yang and R. A. Palmer, The Natural Optical Activity of Tris(Ethylenediamine)Metal(II) Nitrates V. The Single Crystal Circular Dichroism Spectrum of Ni $(en)_3(NO_3)_2$, *J. Chin. Chem. Soc.*, 1978, **25**, 195–201.

57 P. Comba, M. Großhauser, R. Klingeler, C. Koo, Y. Lan, D. Müller, J. Park, A. Powell, M. J. Riley and H. Wadepohl, Magnetic Interactions in a Series of Homodinuclear Lanthanide Complexes, *Inorg. Chem.*, 2015, **54**, 11247–11258.

58 F. S. Richardson, Selection rules for lanthanide optical activity, *Inorg. Chem.*, 1980, **19**, 2806–2812.